Journal of the American College of Cardiology Vol. 55, No. 12, 2010

Published by Elsevier Inc.
ISSN 0735-1097/10/$36.00
doi:10.1016/j.jacc.2009.11.056

PRE-CLINICAL RESEARCH

Effect of an Antimicrobial Agent on Atherosclerotic Plaques

Assessment of Metalloproteinase Activity by Molecular Imaging

Satoru Ohshima, MD, PHD,* Shinichiro Fujimoto, MD, PHD,* Artiom Petrov, PHD,* Hironori Nakagami, MD, PHD,† Nezam Haider, PHD,* Jun Zhou, MD,* Nobuhiro Tahara, MD, PHD,* Mariana Kiomy Osako, PHD,† Ai Fujimoto, MD, PHD,* Jie Zhu, MD,* Toyoaki Murohara, MD, PHD,† D. Scott Edwards, PHD,‡ Navneet Narula, MD,* Nathan D. Wong, PHD,* Y. Chandrashekhar, MD,§ Ryuichi Morishita, MD, PHD,† Jagat Narula, MD, PHD*

Irvine, California; Osaka, Japan; North Billerica, Massachusetts; and Minneapolis, Minnesota

Objectives Technetium-99m–labeled matrix metalloproteinase inhibitor (MPI) was used for the noninvasive assessment of matrix metalloproteinase (MMP) activity in atherosclerotic plaques after minocycline (MC) intervention.

Background MMP activity in atherosclerosis contributes to plaque instability. Some antimicrobial agents may attenuate MMP activity.

Methods Atherosclerotic lesions were produced in 38 rabbits with a high cholesterol diet for 4 months; 5 groups of rabbits, in the fourth month, received fluvastatin (FS) (n = 6), low-dose MC (n = 7), high-dose MC (n = 7), a combination of low-dose MC and FS (n = 6), or no intervention (n = 12); 8 unmanipulated rabbits were used as disease controls. Micro–single-photon emission computed tomography imaging was performed in all animals after intravenous MPI administration, followed by pathologic characterization of the aorta. A cell culture study evaluated the effect of MC on MMP production by activated human monocytes.

Results MPI uptake was visualized best in untreated atherosclerotic animals (percent injected dose per gram MPI uptake, 0.11 ± 0.04%). MPI uptake was reduced in the FS (0.06 ± 0.01%; $p < 0.0001$), high-dose MC (0.05 ± 0.01%; $p < 0.0001$), and MC-FS (0.05 ± 0.005%; $p < 0.0001$) groups. Low-dose MC did not resolve MPI uptake significantly (0.08 ± 0.02; $p = 0.167$). There was no incremental benefit of the combination of MC and FS. MPI uptake showed a significant correlation with plaque MMP-2, and MMP-9 activity. MMP-9 release from tumor necrosis factor-α–activated macrophages was abrogated by incubation with MC.

Conclusions Molecular imaging of MMP activity in atherosclerotic plaque allows for the study of the efficacy of therapeutic interventions. MC administration resulted in substantial reduction in plaque MMP activity and histologically verified plaque stabilization. MC was found to be equally effective as FS. (J Am Coll Cardiol 2010;55:1240–9)

Disruption of a thin fibrous cap in an atherosclerotic plaque is the pathologic substrate responsible for at least two thirds of the acute coronary events. The atherosclerotic plaques that are vulnerable to rupture, usually demonstrate large plaque and necrotic core volumes, which initially is accommodated by positive remodeling of the involved vascular segment and the overlying thin fibrous cap which is substantially inflamed (1,2). Various cytokines, including matrix metalloproteinases (MMPs), secreted from macrophages and smooth muscle cells (SMCs) in atherosclerotic plaques result in collagen and elastin degradation (3). Increased plaque MMP activity contributes to fibrous cap attenuation and expansive vessel remodeling (4–7). Therefore, MMP activity traditionally has been considered a potential target for plaque stabilization.

Treatment with statins substantially resolves MMP expression in experimentally induced atherosclerotic lesions. We observed a 50% reduction in the plaque MMP activity in

From the *University of California Irvine School of Medicine, Irvine, California; †Osaka University Graduate School of Medicine, Osaka, Japan; ‡Lantheus Medical Imaging, North Billerica, Massachusetts; and the §University of Minnesota, Minneapolis, Minnesota. The study was supported entirely by National Institutes of Health grant R01 (HL 078681) to Dr. Narula. Dr. Edwards is an employee of Lantheus Medical Imaging, which supplied the imaging tracer for the study. Dr. Narula has received RP-805 from Lantheus Medical Imaging and fluvastatin from Tanabe Pharmaceutical Company (Japan). Drs. Ohshima and Fujimoto contributed equally to this work.

Manuscript received February 7, 2009; revised manuscript received November 16, 2009, accepted November 19, 2009.

statin-treated animals (8). Antimicrobial agents, such as tetracycline and its derivatives, demonstrate substantial MMP inhibitory activity, including suppression of collagenases, gelatinases, and stromelysins in vitro (9,10). These agents have been used to minimize tissue degradation in aortic aneurysms (11–14) and arthritis (15–18), and also inhibit tumor cell invasion and metastasis (19,20). In addition, tetracyclines also have been reported to exert an antiapoptotic effect by preventing cytochrome C release from mitochondria, and therefore caspase-3 activation (21). As such, minocycline (MC) has been used successfully to delay progression of amyotrophic lateral sclerosis in mice and to reduce mortality in a Huntington disease mouse model (21,22). Tetracyclines also inhibit production of inflammatory cytokines, such as interleukin-1 and interleukin-6, neutrophil elastase, relative oxygen intermediates, and MMP, and have been used effectively in acute lung injury and chronic inflammatory diseases (23,24).

The present study was performed to evaluate the efficacy of MC in inhibition of MMP activity in atherosclerotic plaques. The efficacy of MC was compared with that of fluvastatin (FS). Technetium (Tc) 99m–labeled broad-spectrum matrix metalloproteinase inhibitor (MPI) was administered for the in vivo assessment of MMP activity in atherosclerotic plaques. Histologic and biochemical characterization of explanted aortic tissue was performed. A cell culture study also evaluated the effect of MC on MMP production by activated human monocytes and compared the effect of MC with that of incubation with FS.

Methods

In vivo study design. The present study was performed in 46 New Zealand white rabbits (Fig. 1). Experimental atherosclerotic lesions were induced in 38 of 46 rabbits by balloon de-endothelialization of the infradiaphragmatic aorta, and high cholesterol (HC) diet for 4 months. These 38 atherosclerotic rabbits were divided in 5 groups: 12 were evaluated without drug intervention as treatment control (Rx-control) group, 7 received low-dose MC (1.5 mg/kg orally once daily), 7 received high-dose MC (3 mg/kg orally once daily), 6 received FS (1 mg/kg orally once daily), and 6 received a combination of low-dose MC and FS (MC-FS) in their last month of HC feeding. The remaining 8 of 46 rabbits were left unmanipulated, received normal rabbit chow, and were investigated as disease control (Dz-control) group. The MPI used for imaging in the present study (RP-805) was provided by the Research and Development Division of Lantheus Medical Imaging (North Billerica, Massachusetts); the structure of MPI was reported previously (8). A portion of this compound binds

Abbreviations and Acronyms

CT = computed tomography
FS = fluvastatin
HC = high cholesterol
MC = minocycline
MMP = matrix metalloproteinase
MPI = matrix metalloproteinase inhibitor
SMC = smooth muscle cell
SPECT = single-photon emission computed tomography
Tc = technetium
%ID/g = percent injected dose per gram

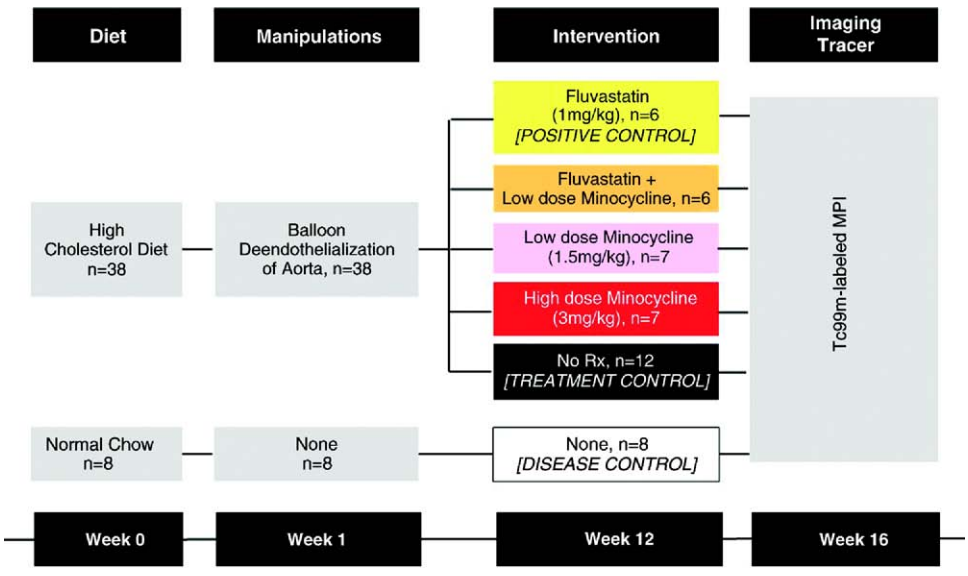

Figure 1 Experimental Design of Study

A broad matrix metalloproteinase (MMP) inhibitor (MPI) radiolabeled with technetium (Tc) 99m was used for noninvasive molecular imaging of MMP activity (as a surrogate marker of plaque instability) in an experimental model of atherosclerosis in New Zealand white rabbits. The effect of minocycline on plaque MMP activity was assessed. Three control groups were used: 1) normal rabbits (disease controls); 2) untreated animals (treatment controls); and 3) rabbits treated with a statin (positive controls or gold standard for reduction in MMP activity). All imaging was performed at 4 months, and pharmaceutical intervention was performed in the last (fourth) month.

to the exposed catalytic domain of MMP. On the basis of enzymatic assays, MPI binds specifically to a broad range of active MMP and not to other proteases. MPI shows an enzyme inhibitory profile of 6.5 nM, 14 nM, <6.4 nM, 7.4 nM, <6.0 nM, 7.3 nM, 27 nM, and 95 nM for MMP-2, MMP-3, MMP-7, MMP-9, MMP-12, MMP-13, ADAM-10, and ADAM-17, respectively (8). The MPI was radiolabeled with Tc-99m. After intravenous administration of MPI, micro–single-photon emission computed tomography (SPECT)/micro-computed tomography (CT) imaging was performed for noninvasive localization of the radiotracer (8). Subsequently, the quantitative MPI uptake in atherosclerotic plaques was determined and was correlated with biochemically and histopathologically verified MMP-2 activity, MMP-9 activity, or both.

Experimental model of atherosclerosis. Male New Zealand white rabbits (2.5 to 3.5 kg, Western Oregon Breeding Laboratories, Philomoth, Oregon) were fed an HC diet containing 0.5% cholesterol and 6% peanut oil. One week later, balloon de-endothelialization of the abdominal aorta was performed using a 4-F Fogarty embolectomy catheter (12-040-4F, Edwards Lifesciences, Irvine, California) as described previously (25). Under general anesthesia with a mixture of ketamine and xylazine (100 mg/ml, prepared in a 10:1 ratio and using 1.5 to 2.5 ml subcutaneously), the right femoral artery was exposed surgically, and an embolectomy catheter was introduced through a small arteriotomy and was advanced up to the level of the diaphragm in the abdominal aorta. The catheter was inflated and pulled antegrade to the bifurcation of the aorta for endothelial denudation. The denudation process was repeated 3 times, and the catheter was removed. The femoral artery was ligated, and the incision site was closed. The HC diet was continued for 15 more weeks. This protocol conformed to the Guidelines for the Care and Use of Laboratory Animals by the National Institute of Health (NIH Publication no. 85-23, revised 1996) and was approved by the Institutional Laboratory Animal Care and Use Committee at University of California, Irvine.

Imaging protocol and quantitative assessment of the tracer uptake. Based on the enzymatic assays reported previously (8,26), the targeting agent MPI binds specifically to activated catalytic domains of broad range of active MMP species and not to other proteases. For radiolabeling, 30 μg RP805 was incubated with 90 mCi/ml Tc-99m pertechnetate at 100°C for 10 min as described previously (8,26). High-pressure liquid chromatography analysis revealed product purity of more than 97%. The injected dose of Tc-MPI was 6.80 ± 0.10 mCi per animal.

As reported previously (8), the radionuclide imaging was performed under general anesthesia with 2.0% of isoflurane. In vivo radionuclide imaging of MPI was performed immediately after tracer injection for blood pool image of the aorta and 4 h later for the tracer uptake in the target lesions, using a dual-head micro-SPECT gamma camera equipped with micro-CT (X-SPECT, Gamma Medica, Inc., Northridge, California). SPECT images of the aorta were acquired in 32 steps of 20 s (at 0 h image) or 120 s (at 4 h image) per projection, at 140 keV photopeak of Tc-99m with 15% windows, using a low-energy, high-resolution parallel-hole collimator. SPECT images were acquired in 64 × 64-matrix format. After SPECT image acquisition, micro-CT imaging was performed using an X-ray tube operating at 50 kVp and 0.6 mA for 2.5 s of 256 directions for 360° rotation. Then, the micro-SPECT and the micro-CT images were fused, allowing scintigraphic and anatomic information in all tomographic scans in the 3 different spatial axes.

After in vivo imaging, animals were killed with an overdose of sodium pentobarbital (120 mg/kg). The aortas were harvested for ex vivo imaging and gamma counting of tissue for quantitative assessment of tracer uptake. Ex vivo images of the aorta were acquired for 15 min. Then, entire aortas were segmented at 1-cm intervals, weighed, and gamma counted in an automatic well-type gamma counter (PerkinElmer-Wallac, Inc., Gaithersburg, Maryland) for calculation of the percent total injected dose MPI uptake per gram aorta tissue (%ID/g). Atherosclerotic samples were preserved for histological and immunohistochemical investigation, and MMP activity assays.

Histologic and immunohistochemical study of atherosclerotic lesions. One-half of every 1-cm aortic segment was frozen for MMP activity assay. The remaining half was fixed overnight for histologic study with 4% paraformaldehyde in phosphate-buffered saline, pH 7.4, at 4°C, and stored in phosphate-buffered saline with 0.02% sodium azide at 4°C. The fixed tissue segments were paraffin embedded, and 4-μm thick sections were obtained. The tissue sections then were deparaffinized for histologic assessment and the sections were stained with hematoxylin and eosin, and Movat pentachrome. SMCs were identified using a primary antibody against α-actin isotypes (MAB1420, 1:10K, R&D System, Minneapolis, Minnesota) and macrophages by using RAM-11 (M-0633, 1:3K, DAKO, Carpinteria, California). For the detection of MMP expression, monoclonal MMP-2 (gelatinase-A, IM53, 1:52K, Calbiochem, Gibbstown, New Jersey) and monoclonal MMP-9 (gelatinase-B, IM37, 1:15K, Calbiochem) antibodies were used. A color reaction was developed by incubation with diaminobenzamine (DAB, brown color, SK-4100, Vector) for α-actin and RAM-11 antibodies, and the Catalyzed Signal Amplification II kit (DAKO) was used for the staining of the MMP-2 and -9. The sections were counterstained with Gill's hematoxylin. As a negative control for the immunostaining procedure, sections were incubated in parallel without primary antibody or with control immunoglobulin G. For the assessment of the immunopositive area, stained tissue sections were observed under appropriate magnification (Carl Zeiss, Thornwood, New York), and the images were captured with a high-resolution digital camera (Axiocam, 1,300 × 1,030 pixels, Carl Zeiss) using Axiovision 3.1 software. Digital images were

analyzed using Image-Pro Plus 5.0 (Media Cybernetics, Bethesda, Maryland). The percent immunopositive area (immunopositive area/total intimal area × 100) was determined for all markers by averaging several images per section that covered the entire plaque. All quantitative comparisons for a given marker were performed on the sections stained simultaneously.

MMP activity assay. The frozen tissue samples were homogenized in 1 ml lysis buffer (50 mM Tris-HCl, pH 7.6, 150 mM NaCl, 1 mM phenyl-methanesulfonyl-fluoride, 10 μg/ml Aprotinin, 10 μg/ml Leupeptin, 1 mM 1,4-Dithio-DL-threitol). After 30 min of incubation in ice, homogenates were centrifuged at 4° C for 15 min at 10,000 × g. Supernatants were transferred into fresh tubes and protein concentrations were determined (BIO-RAD Protein Assay, Hercules, California) and were equalized for all samples. Enzyme-linked immunosorbent assays were performed for the supernatant for pro and active MMP-9 enzymatic activity. Twenty-five micrograms of total proteins were used for the MMP assay, and all samples were analyzed in triplicate. The MMP-9 Biotrak Activity Assay System (Amersham Bioscience Corp., Piscataway, New Jersey) was used according to the manufacturer's protocol.

In vitro cell culture study investigating production of MMP. CELL CULTURE. THP-1 cells (American Type Culture Collection, Rockville, Maryland) were cultured in RPMI Medium 1640 (Invitrogen, Carlsbad, California) enriched with 10% fetal bovine serum (Cambrex Bio Sciences Walkersville, Inc., Walkersville, Maryland) with 100 U/ml penicillin and 100 mg/ml streptomycin at 37°C with 5% CO_2. Cell viability was measured using MTS [3-(4,5-dimethylthiazol-2-yl)-5-(3-carboxymethoxyphenyl)-2-(4-sulfophenyl)-2H-Tetrazolium] assay, and were seeded on a 96-well plate (5×10^3 cells/well) in a volume of 100 μl and were incubated for 24 h with FS, MC, and 10 ng/ml of tumor necrosis factor-alpha (Peprotech, London, United Kingdom) in a 2% fetal bovine serum and antibiotics-supplemented smooth muscle cell basal medium (Cambrex Bio Sciences Walkersville, Inc.). The medium was replaced with 100 μl smooth muscle cell basal medium plus 5% fetal bovine serum supplemented with antibiotics and 10 μl Cell Titer 96 One Solution Reagent (Promega, Madison, Wisconsin). Absorbance at 490 nm was measured after 1 h of incubation at 37° C with 5% CO_2.

RELATIVE QUANTIFICATION OF MMP-9 mRNA OF MACROPHAGES BY REAL-TIME PCR. Total ribonucleic acid (RNA) was isolated using an Agilent Total RNA Isolation Mini Kit (Agilent Technologies, Wilmington, Delaware), and the complementary deoxyribonucleic acid reaction was performed using a High-Capacity cDNA Archive kit (Applied Biosystems, Foster City, California) according to the procedures recommended by the manufacturer. Each complementary deoxyribonucleic acid sample was analyzed for MMP-9 and 18S expression by real-time quantitative polymerase chain reaction using the fluorescent TaqMan 5′ nuclease assay. Oligonucleotide primers were used according to the identification MMP-9: Hs00234579 and Human Euk 18S rRNA (Applied Biosystems, Warrington, United Kingdom). The 5′ nuclease assay polymerase chain reactions were performed in a MicroAmp Optical 96-well Reaction Plate using the ABI PRISM 7700 Sequence Detection System (ABI Prism Applied Biosystems, Foster City, California). Levels of MMP-9 and 18S mRNA were quantified by comparison of the fluorescence generated by

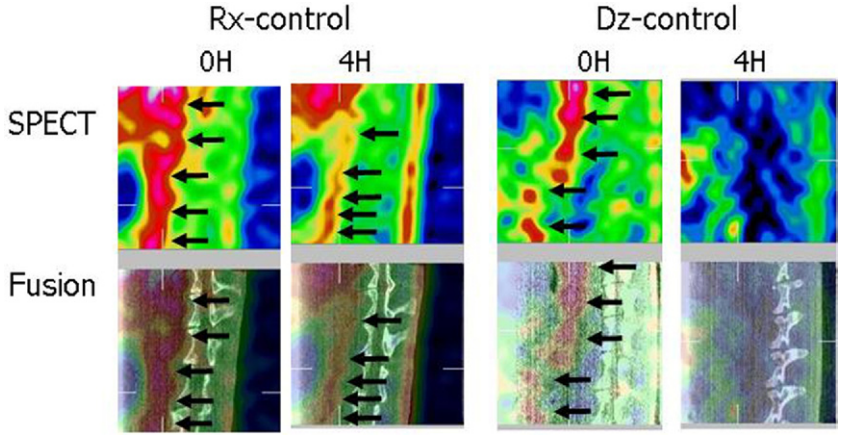

Figure 2 **In Vivo Images of Atherosclerotic Lesion in the No Drug Intervention Atherosclerotic Rabbits (Rx-Control) and Unmanipulated Normal Animals (Dz-Control) Groups**

Each image is shown in 2 × 2 format in a sagittal projection. The **upper row** displays micro–single-photon emission computed tomography (SPECT) images, and the lower row demonstrates fusion of micro-SPECT and micro-computed tomography images. The **left column** shows an image immediately after the radiotracer injection (0H) and represents the blood pool image in the aorta. The **right column** shows images taken at 4 h (4H) after tracer injection, representing the tracer uptake in the target lesions. In both the Rx-control and Dz-control groups, blood pool images in the abdominal aorta in front of the vertebral column are observed clearly. In 4H images, maximum matrix metalloproteinase inhibitor uptake is observed in the abdominal atherosclerotic lesion of the Rx-control animal; no tracer uptake is observed in the aortic region of the Dz-control animal.

each sample with that of a serially diluted standard and were normalized by the level of 18S expression in each individual sample.

Statistical methods. We determined that 6 animals in each treatment intervention group would be sufficient to detect a 50% lower MPI uptake in a treated compared with untreated (Rx-control) group with 80% power at a 1-tailed $p = 0.05$, a 50% reduction in activity was based on our previously reported observation (24) evaluating the efficacy of FS in modulating plaque characteristics. As such, similar animal group sizes for 6 study groups would be able to detect a 15%, 25%, 35%, and 40% reduction in MMP activity with a power of 39%, 77%, 88%, and 94% based on a 2-tailed $\alpha = 0.05$ analysis of variance. On application of Kolmogorov-Smirnov (with Lilliefors significance correction) and Shapiro-Wilk tests, the study data were found to be normally distributed. However, because of the small sample size, we applied the nonparametric Kruskal-Wallis test followed by the Mann-Whitney *U* test for pairwise significance, if any, using the SPSS package version 17 (SPSS, Inc., Chicago, Illinois). To evaluate the correlation between %ID/g MPI uptake and histologic findings (including MMP-2 and -9) of atherosclerotic plaques, Spearman's rank correlation coefficients were computed.

Results

Imaging of MMP activity in atherosclerotic lesions. In all groups, immediately after intravenous administration of radiotracer, noninvasive micro-SPECT images revealed blood pool activity in front of the vertebral column, verified by micro-CT (Fig. 2). The blood pool activity gradually receded over time, and target localization in the aorta became evident. The lesions were visualized best in 4-h images in Rx-control (untreated) animals. In unmanipulated Dz-control animals, no uptake was seen at 4 h (Fig. 2). The lesions were less apparent in 4-h images in the low-dose MC group (Fig. 3), and no uptake was seen in the high-dose MC group (Fig. 2). The uptake in the high-dose MC group was comparable with that of the FS group (Fig. 3). After completion of each in vivo imaging session, the animal was killed and the aorta was harvested. Explanted

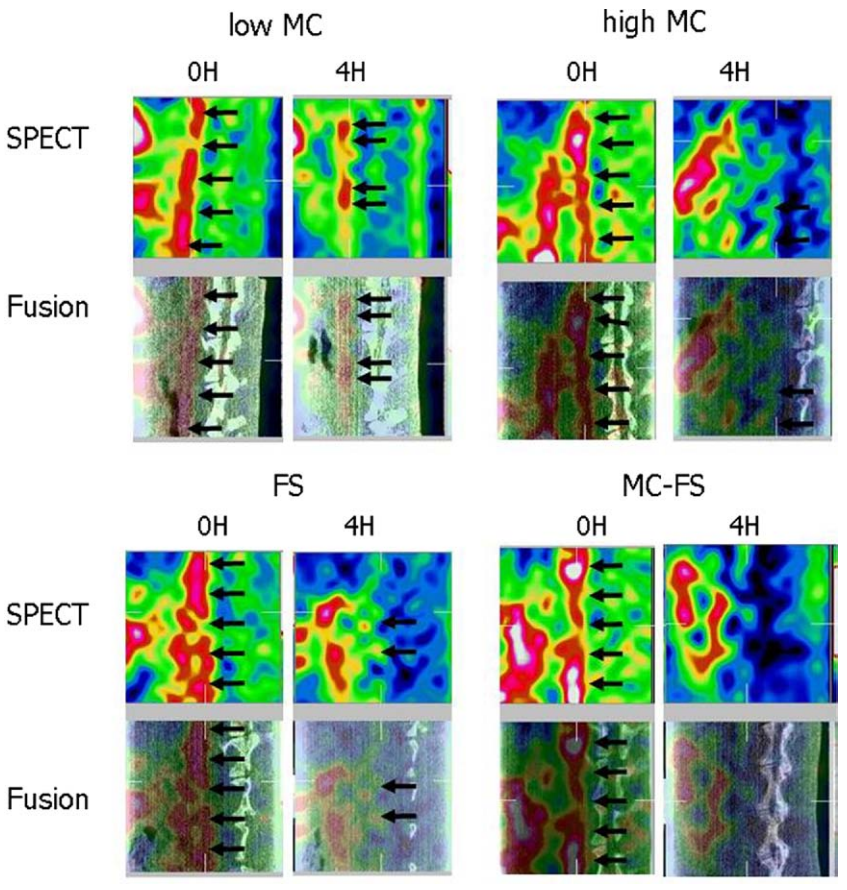

Figure 3 In Vivo Images of Atherosclerotic Lesion in Drug Intervention Groups

Micro–single-photon emission computed tomography (SPECT) and micro-SPECT/micro-computed tomography fusion images in sagittal projections in drug intervention groups are shown at 0 h (0H) and 4 h (4H) after administration of radiotracer. In high MC, FS, and MC-FS intervention groups, matrix metalloproteinase inhibitor uptake is reduced significantly. FS = fluvastatin; MC = minocycline.

aorta then was subjected to ex vivo imaging (Fig. 4). Ex vivo images revealed the most intense uptake in atherosclerotic abdominal lesions in the Rx-control group and no uptake in the Dz-control groups. The tracer uptake in ex vivo images was reduced variably in animal groups receiving MC or FS compared with the Rx-control groups. The ex vivo images confirmed the in vivo distribution of MPI.

Quantitative MPI uptake in atherosclerotic lesions. The maximum %ID/g MPI uptake in the abdominal atherosclerotic lesions was observed in the Rx-control group (0.11 ± 0.04%, $z = -3.55$, $p < 0.0001$). There was a substantial decrease in the quantitative uptake in FS (0.06 ± 0.01%, $z = -3.37$, $p < 0.0001$), high-dose MC (0.05 ± 0.01%, $z = -3.55$, $p < 0.0001$), and low-dose MC-FS (0.05 ± 0.005%, $z = -3.37$, $p < 0.0001$) groups as compared with the Rx-control group. The uptake in the low-dose MC group (0.08 ± 0.02%, $z = -1.47$, $p = 0.167$) was not significantly different from that of the untreated group (Fig. 4). Addition of low-dose MC to FS did not offer incremental benefit in reduction of MPI uptake, and no significant differences were observed among the high-dose MC, FS, and MC-FS groups. The Dz-control abdominal aortas (0.02 ± 0.004%) showed minimal background activity compared with those of untreated animals ($z = -3.7$, $p < 0.0001$).

Histopathologic and immunohistochemical characterization of atherosclerotic lesions. Variable extent of intimal thickening and fibroatheroma were observed in each atherosclerotic animal. The neointimal lesions in the Rx-control group showed maximum macrophage density and greatest MMP-2 and -9 activity (Fig. 5A). The macrophage density and the MMP expression were reduced in the MC (Fig. 5A), FS, and MC-FS groups. Percent macrophage area was significantly greater in the Rx-control group (3.59 ± 2.09%) than in the FS (1.39 ± 0.60%, $p = 0.0003$), low-dose MC (0.82 ± 0.41%, $p = 0.003$), high-dose MC (0.79 ± 0.14%, $p = 0.0004$), or MC-FS (0.94 ± 0.41%, $p = 0.0004$) groups (Fig. 5B). Similarly, MMP-2 and MMP-9 immunopositive areas by quantitative histopathologic analysis were significantly larger in the Rx-control group (0.89 ± 0.33% and 0.18 ± 0.13%, respectively) compared with the FS (0.44 ± 0.09%, $p = 0.0003$ and 0.08 ± 0.04%, $p = 0.01$, respectively), low-dose MC (0.52 ± 0.06%, $p = 0.006$ and 0.08 ± 0.02%, $p = 0.006$, respectively), high-dose MC (0.52 ± 0.07%, $p = 0.007$ and 0.06 ± 0.03%, $p = 0.003$, respectively), and MC-FS (0.39 ± 0.16%, $p = 0.006$ and 0.09 ± 0.03%, $p = 0.008$, respectively) groups (Fig. 5B). A significant correlation was observed between quantitative MPI uptake and immunopositive MMP-2 ($r = 0.61$, $p = 0.007$) and MMP-9 ($r = 0.68$, $p = 0.07$) areas (Fig. 5C). There was no significant correlation between MPI uptake and macrophage ($r = 0.25$; $p = 0.28$) and SMC ($r = 0.26$; $p = 0.28$) density (Fig. 5C).

MMP activity assay of aortic sample and cell culture studies for MC effect. Biochemically verified MMP-9 activity also was significantly higher in the Rx-control group (0.450 ± 0.033 ng/50 μg sample) compared with the Dz-control group (−0.098 ± 0.006 ng/50 μg, $p < 0.0001$). Active MMP-9 levels significantly decreased in the FS (0.248 ± 0.001 ng/50 μg, $p < 0.0001$), low-dose MC (0.344 ± 0.01 ng/50 μg, $p < 0.0001$), high-dose MC (0.123 ± 0.002 ng/50 μg, $p < 0.0001$), and MC-FS (0.260 ± 0.002 ng/50 μg, $p < 0.0001$) groups (Fig. 6).

MMP-9 expression in tumor necrosis factor-alpha–stimulated macrophages was determined by a real-time polymerase chain reaction, and a significant reduction of MMP-9 expression in macrophages was observed by FS, higher concentration of MC, and combination of MC and FS (Fig. 7).

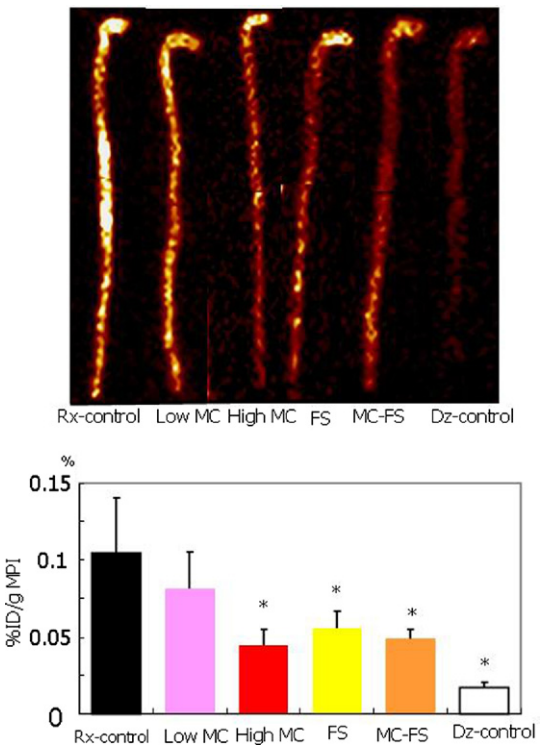

Figure 4 Ex Vivo Images of Aortas and Quantitative MPI Uptake in Various Study Groups

(Top) Ex vivo images showing the most prominent matrix metalloproteinase inhibitor (MPI) uptake in an abdominal atherosclerotic lesion of a no drug intervention (Rx-control) animal. Uptake is reduced in each drug intervention group. No MPI uptake is observed in the unmanipulated normal animal (Dz-control). **(Bottom)** Bar graph showing quantitative MPI uptake in the abdominal aorta of various study groups. MPI uptakes are significantly lower in high-dose minocycline (MC), fluvastatin (FS), and low-dose MC and FS drug intervention groups as compared with the Rx-control (i.e., untreated) group. *$p < 0.0001$.

Discussion

In a rabbit model of atherosclerosis produced by balloon de-endothelialization of the aorta and an HC diet, orally administered MC resulted in a markedly decreased production of MMP as identified by molecular imaging with a radiolabeled broad-spectrum MPI. Histopathologic examination confirmed the correlation of MMP-2 and MMP-9

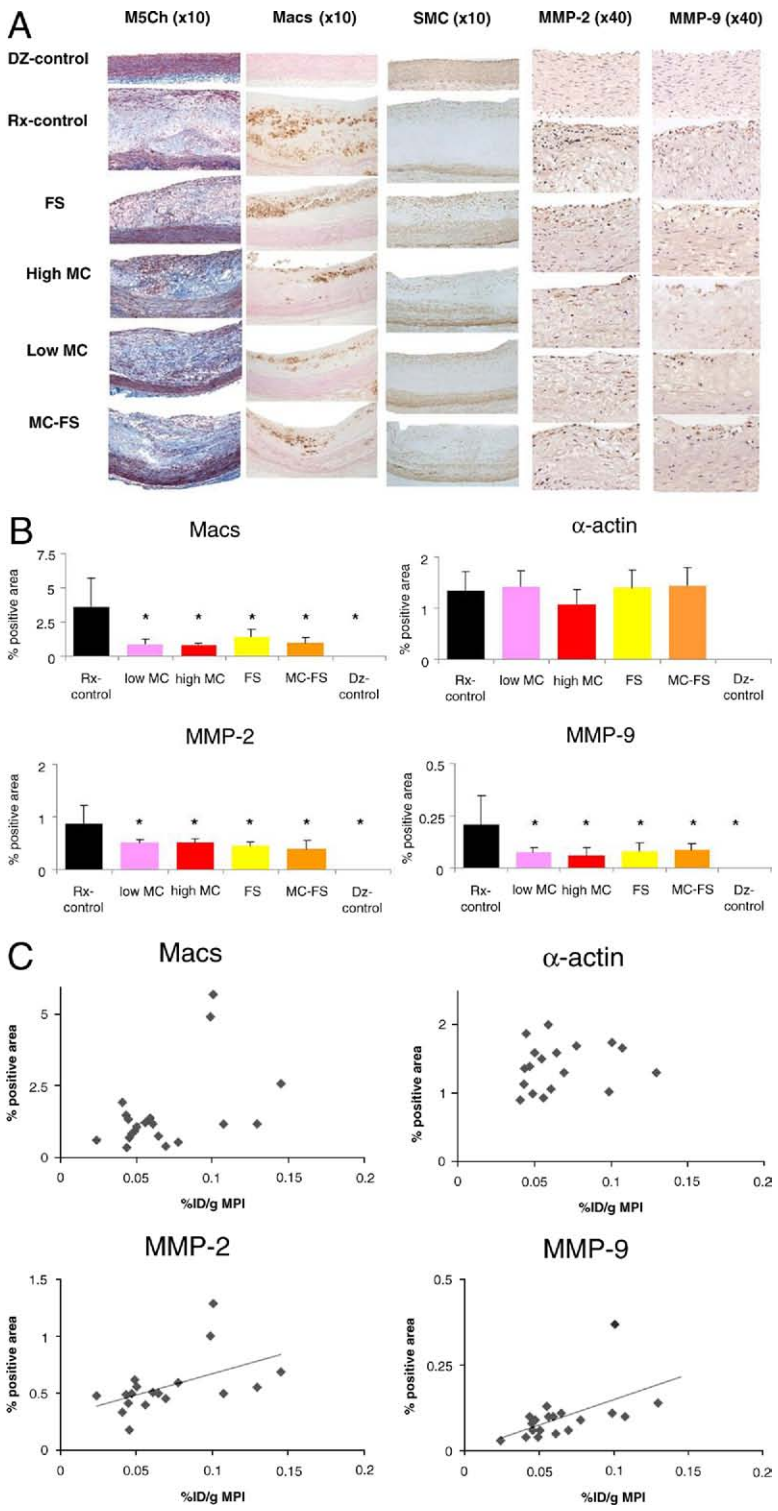

Figure 5 **Histologic and Immunohistochemical Characterization of Atherosclerotic Lesions**

(A) Movat pentachrome (M5Ch) staining and immunohistochemical staining of atherosclerotic lesions in various study groups using RAM-11 (macrophages), anti α-actin antibody (SMC), and anti-matrix metalloproteinase (MMP)-2 and -9 antibody are shown. **(B)** The immunopositive areas are evaluated quantitatively in these animals. The atherosclerotic lesions of no drug intervention (Rx-control) animals show maximal neointimal lesion, highest density of macrophages, and highest concentrations of MMP-2 and -9. In each drug intervention group, macrophage density and MMP-2, and MMP-9 concentrations are reduced significantly. *$p < 0.01$. **(C)** Significant correlations are observed between quantitative MMP inhibitor (MPI) uptake and MMP-2 ($r = 0.61$; $p = 0.007$) and MMP-9 ($r = 0.68$; $p = 0.07$) concentrations. Dz-control = unmanipulated normal animal; FS = fluvastatin; MC = minocycline; %ID/g = percent total injected dose per gram tissue.

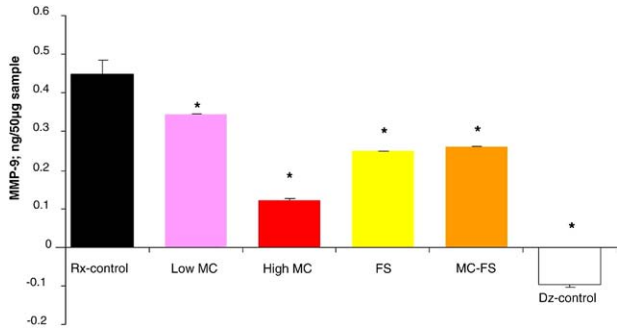

Figure 6 **Quantitative MMP-9 Activity Assay in Aortic Samples in Various Study Groups**

Highest MMP-9 activity is observed in the no drug intervention (Rx-control) group. In all drug intervention groups, significant reductions are observed. *$p < 0.0001$. Dz-control = unmanipulated normal animal; FS = fluvastatin; MC = minocycline.

expression with %ID/g MPI uptake. MC-treated animals revealed reduced expression of MMP-2 and MMP-9. The histologic features were suggestive of plaque stabilization; the efficacy of MC also was confirmed by MMP activity assays. In addition, MC inhibited MMP-9 expression by activated macrophages in cell culture studies. Using the same methodology and protocol, we recently reported approximately 50% resolution of MMP activity after FS treatment (8). FS intervention was associated with 66% reduction in macrophage infiltration and 50% to 75% lower MMP-2 and -9 activity. In the present study, %ID/g MPI uptake was reduced by MC in a dose-dependent manner. Whereas low-dose MC statistically insignificantly resolved MPI uptake, high-dose MC was at least as effective as statins. The combination of low-dose MC with FS did not reduce the MPI uptake further.

Although FS-related decrease in MMP production in atherosclerotic plaque is known (27), the mechanism of plaque stabilization by the tetracyclines is not clear. Tetracyclines may exert nonselective MMP inhibitory property by directly binding to Zn^{2+} or Ca^{2+} and may block the active site or may induce conformational change to render the proenzyme susceptible to fragmentation (28,29). Tetracyclines also may influence the transcriptional or translational process of the MMP synthesis (30–33). They have been shown to attenuate MMP-2 and -9 activity in the aortic wall (32–34). Both clinical and animal experimental studies have revealed that tetracyclines decrease serum inflammatory markers and cytokines, as well as MMP in arteriosclerotic diseases (35,36). Experiments using chemically modified tetracyclines have demonstrated that MMP suppression and anti-inflammatory action occurs at a different molecular level from that for antibiotic activity (23,33). Tetracyclines also exert antiapoptotic properties by inhibiting caspase-1 and caspase-3 and by reducing cytochrome C leakage from mitochondria (21,37). In atherosclerotic lesions, MC also may inhibit apoptosis of macrophages, which is associated with MMP-9 release (38).

In the present study, MC suppressed MMP expression and contributed to plaque stabilization. This finding of MMP suppression is consistent with previous reports (34). We used 3 mg/kg daily of minocycline for the high-dose group and 1.5 mg/kg daily for the low-dose group. On conversion to clinical scale, the low-dose MC corresponds to 100 mg/day and the high-dose MC corresponds to 200 mg/day. Such doses have been found to be clinically effective in carotid artery atherosclerosis (39) and Takayasu disease (39,40). Therefore, the doses of MC used in the present study are sufficient to be therapeutically effective. However, blood concentration of 2.7 to 11.9 μg/ml was required for 45% to 60% inhibition of aortic aneurysm growth in a mouse model, which translates to the blood concentration of the patients receiving 200 mg/day of doxycycline for 3 months (41). The toxicity of tetracyclines is also dose dependent. From the standpoint of safety in long-term clinical use, a lower dose of doxycycline, 20 to 40 mg/day, has been reported to be safe (35,42), which may not show acceptable results in aortic disease. In our study, low-dose administration of MC (equivalent to 100 mg doxycycline/day) demonstrated insufficient MMP suppression, and the lack of synergistic effect of MC and FS was inexplicable. Because intervention with high-dose MC during acute myocardial infarction substantially attenuates myocardial damage (43), it is logical to propose that short-term use of MC may contribute to plaque stabilization and may help to prevent recurrence of vascular events. This should be particularly attractive if an MPI (such as MC) is acutely as effective in plaque stabilization as apoptosis inhibitors (44). The efficacy of MC also offers credence to the emerging role of antibiotics in prevention of acute coronary syndromes (45,46).

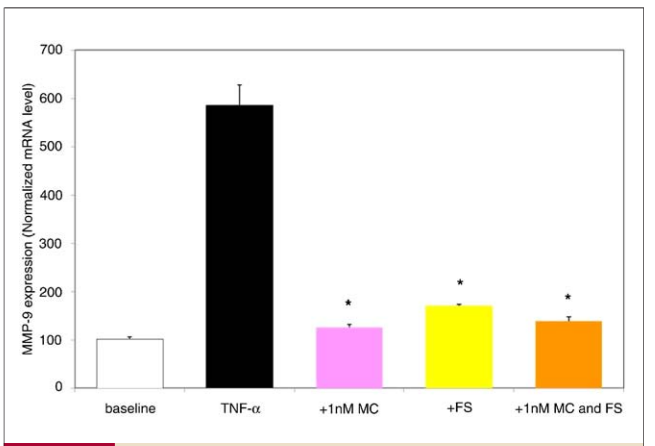

Figure 7 **Cell Culture Studies of MMP-9 Production by Macrophage**

The effect of fluvastatin (FS), minocycline (MC), or their combination on MMP-9 expression in activated macrophage is demonstrated by real-time polymerase chain reaction. Significant reductions of MMP-9 expression in activated macrophage are observed by FS, MC, and their combination. *$p < 0.0001$ versus tumor necrosis factor (TNF)-alpha stimulation.

Study limitations. Although the study findings are intriguing, they support the role of antibiotics in the prevention of coronary events. More robust experimental evidence is needed, including studies with a larger sample size, a greater spectrum of antibiotics, and a wider dose range for developing a case for targeted clinical investigation. Further, in addition to reduction in MMP activity, a more direct evidence of plaque stabilization would be required. Finally, it will be important to exclude infectious cause in the animal experiments to propose a nonmicrobial role of antibiotics in coronary disease.

Conclusions

The present study shows the feasibility of molecular imaging for demonstrating the efficacy of therapeutic intervention targeted at MMP activity in atherosclerotic plaques. This study reveals an MMP inhibitory activity of high-dose MC administration for possible plaque stabilization.

Reprints requests and correspondence: Dr. Artiom Petrov, Division of Cardiology, University of California Irvine School of Medicine, Medical Science I, C-116, UCI Main Campus, Irvine, California 92697. E-mail: adpetrov@uci.edu.

REFERENCES

1. Virmani R, Kolodgie FD, Burke AP, Farb A, Schwartz SM. Lessons from sudden coronary death: a comprehensive morphological classification scheme for atherosclerotic lesions. Arterioscler Thromb Vasc Biol 2000;20:1262–75.
2. Virmani R, Burke AP, Farb A, Kolodgie FD. Pathology of the vulnerable plaque. J Am Coll Cardiol 2006;47:C13–8.
3. Visse R, Nagase H. Matrix metalloproteinases and tissue inhibitors of metalloproteinases: structure, function, and biochemistry. Circ Res 2003;92:827–39.
4. Shah PK, Falk E, Badimon JJ, et al. Human monocyte-derived macrophages induce collagen breakdown in fibrous caps of atherosclerotic plaques. Potential role of matrix-degrading metalloproteinases and implications for plaque rupture. Circulation 1995;92:1565–9.
5. Sukhova GK, Schonbeck U, Rabkin E, et al. Evidence for increased collagenolysis by interstitial collagenases-1 and -3 in vulnerable human atheromatous plaques. Circulation 1999;99:2503–9.
6. Galis ZS, Khatri JJ. Matrix metalloproteinases in vascular remodeling and atherogenesis: the good, the bad, and the ugly. Circ Res 2002;90:251–62.
7. Pasterkamp G, Schoneveld AH, Hijnen DJ, et al. Atherosclerotic arterial remodeling and the localization of macrophages and matrix metalloproteases 1, 2 and 9 in the human coronary artery. Atherosclerosis 2000;150:245–53.
8. Fujimoto S, Hartung D, Ohshima S, et al. Molecular imaging of matrix metalloproteinase in atherosclerotic lesions: resolution with dietary modification and statin therapy. J Am Coll Cardiol 2008;52:1847–57.
9. Gilbertson-Beadling S, Powers EA, Stamp-Cole M, et al. The tetracycline analogs minocycline and doxycycline inhibit angiogenesis in vitro by a non-metalloproteinase-dependent mechanism. Cancer Chemother Pharmacol 1995;36:418–24.
10. Golub LM, Ramamurthy NS, McNamara TF, Greenwald RA, Rifkin BR. Tetracyclines inhibit connective tissue breakdown: new therapeutic implications for an old family of drugs. Crit Rev Oral Biol Med 1991;2:297–321.
11. Petrinec D, Liao S, Holmes DR, Reilly JM, Parks WC, Thompson RW. Doxycycline inhibition of aneurysmal degeneration in an elastase-induced rat model of abdominal aortic aneurysm: preservation of aortic elastin associated with suppressed production of 92 kD gelatinase. J Vasc Surg 1996;23:336–46.
12. Curci JA, Petrinec D, Liao S, Golub LM, Thompson RW. Pharmacologic suppression of experimental abdominal aortic aneurysms: a comparison of doxycycline and four chemically modified tetracyclines. J Vasc Surg 1998;28:1082–93.
13. Boyle JR, McDermott E, Crowther M, Wills AD, Bell PR, Thompson MM. Doxycycline inhibits elastin degradation and reduces metalloproteinase activity in a model of aneurysmal disease. J Vasc Surg 1998;27:354–61.
14. Curci JA, Mao D, Bohner DG, et al. Preoperative treatment with doxycycline reduces aortic wall expression and activation of matrix metalloproteinases in patients with abdominal aortic aneurysms. J Vasc Surg 2000;31:325–42.
15. Steinmeyer J, Daufeldt S, Taiwo YO. Pharmacological effect of tetracyclines on proteoglycanases from interleukin-1-treated articular cartilage. Biochem Pharmacol 1998;55:93–100.
16. Greenwald RA, Moak SA, Ramamurthy NS, Golub LM. Tetracyclines suppress matrix metalloproteinase activity in adjuvant arthritis and in combination with flurbiprofen, ameliorate bone damage. J Rheumatol 1992;19:927–38.
17. Greenwald RA, Golub LM, Lavietes B, et al. Tetracyclines inhibit human synovial collagenase in vivo and in vitro. J Rheumatol 1987;14:28–32.
18. Greenwald RA, Golub LM, Ramamurthy NS, Chowdhury M, Moak SA, Sorsa T. In vitro sensitivity of the three mammalian collagenases to tetracycline inhibition: relationship to bone and cartilage degradation. Bone 1998;22:33–8.
19. Fife RS, Sledge GW Jr. Effects of doxycycline on in vitro growth, migration, and gelatinase activity of breast carcinoma cells. J Lab Clin Med 1995;125:407–11.
20. Seftor RE, Seftor EA, De Larco JE, et al. Chemically modified tetracyclines inhibit human melanoma cell invasion and metastasis. Clin Exp Metastasis 1998;16:217–25.
21. Zhu S, Stavrovskaya IG, Drozda M, et al. Minocycline inhibits cytochrome c release and delays progression of amyotrophic lateral sclerosis in mice. Nature 2002;417:74–8.
22. Chen M, Ona VO, Li M, et al. Minocycline inhibits caspase-1 and caspase-3 expression and delays mortality in a transgenic mouse model of Huntington disease. Nat Med 2000;6:797–801.
23. Nieman GF, Zerler BR. A role for the anti-inflammatory properties of tetracyclines in the prevention of acute lung injury. Curr Med Chem 2001;8:317–25.
24. Sapadin AN, Fleischmajer R. Tetracyclines: nonantibiotic properties and their clinical implications. J Am Acad Dermatol 2006;54:258–65.
25. Kolodgie FD, Petrov A, Virmani R, et al. Targeting of apoptotic macrophages and experimental atheroma with radiolabeled annexin V: a technique with potential for noninvasive imaging of vulnerable plaque. Circulation 2003;108:3134–9.
26. Su H, Spinale FG, Dobrucki LW, et al. Noninvasive targeted imaging of matrix metalloproteinase activation in a murine model of postinfarction remodeling. Circulation 2005;112:3157–67.
27. Aikawa M, Rabkin E, Sugiyama S, et al. An HMG-CoA reductase inhibitor, cerivastatin, suppresses growth of macrophages expressing matrix metalloproteinases and tissue factor in vivo and in vitro. Circulation 2001;103:276–83.
28. Golub LM, Lee HM, Ryan ME, Giannobile WV, Payne J, Sorsa T. Tetracyclines inhibit connective tissue breakdown by multiple nonantimicrobial mechanisms. Adv Dent Res 1998;12:12–26.
29. Smith GN Jr, Brandt KD, Hasty KA. Activation of recombinant human neutrophil procollagenase in the presence of doxycycline results in fragmentation of the enzyme and loss of enzyme activity. Arthritis Rheum 1996;39:235–44.
30. Uitto VJ, Firth JD, Nip L, Golub LM. Doxycycline and chemically modified tetracyclines inhibit gelatinase A (MMP-2) gene expression in human skin keratinocytes. Ann N Y Acad Sci 1994;732:140–51.
31. Hanemaaijer R, Visser H, Koolwijk P, et al. Inhibition of MMP synthesis by doxycycline and chemically modified tetracyclines (CMTs) in human endothelial cells. Adv Dent Res 1998;12:114–8.
32. Bendeck MP, Conte M, Zhang M, Nili N, Strauss BH, Farwell SM. Doxycycline modulates smooth muscle cell growth, migration, and matrix remodeling after arterial injury. Am J Pathol 2002;160:1089–95.

33. Islam MM, Franco CD, Courtman DW, Bendeck MP. A nonantibiotic chemically modified tetracycline (CMT-3) inhibits intimal thickening. Am J Pathol 2003;163:1557–66.
34. Pinney SP, Chen HJ, Liang D, Wang X, Schwartz A, Rabbani LE. Minocycline inhibits smooth muscle cell proliferation, migration and neointima formation after arterial injury. J Cardiovasc Pharmacol 2003;42:469–76.
35. Brown DL, Desai KK, Vakili BA, Nouneh C, Lee HM, Golub LM. Clinical and biochemical results of the metalloproteinase inhibition with subantimicrobial doses of doxycycline to prevent acute coronary syndromes (MIDAS) pilot trial. Arterioscler Thromb Vasc Biol 2004;24:733–8.
36. Madan M, Bishayi B, Hoge M, Messas E, Amar S. Doxycycline affects diet- and bacteria-associated atherosclerosis in an ApoE heterozygote murine model: cytokine profiling implications. Atherosclerosis 2007;190:62–72.
37. Scarabelli TM, Stephanou A, Pasini E, et al. Minocycline inhibits caspase activation and reactivation, increases the ratio of XIAP to smac/DIABLO, and reduces the mitochondrial leakage of cytochrome C and smac/DIABLO. J Am Coll Cardiol 2004;43:865–74.
38. Haider N, Hartung D, Fujimoto S, et al. Dual molecular imaging for targeting metalloproteinase activity and apoptosis in atherosclerosis: molecular imaging facilitates understanding of pathogenesis. J Nucl Cardiol 2009;16:753–62.
39. Axisa B, Loftus IM, Naylor AR, et al. Prospective, randomized, double-blind trial investigating the effect of doxycycline on matrix metalloproteinase expression within atherosclerotic carotid plaques. Stroke 2002;33:2858–64.
40. Matsuyama A, Sakai N, Ishigami M, Hiraoka H, Yamashita S. Minocycline for the treatment of Takayasu arteritis. Ann Intern Med 2005;143:394–5.
41. Prall AK, Longo GM, Mayhan WG, et al. Doxycycline in patients with abdominal aortic aneurysms and in mice: comparison of serum levels and effect on aneurysm growth in mice. J Vasc Surg 2002;35:923–9.
42. Walker C, Thomas J, Nango S, Lennon J, Wetzel J, Powala C. Long-term treatment with subantimicrobial dose doxycycline exerts no antibacterial effect on the subgingival microflora associated with adult periodontitis. J Periodontol 2000;71:1465–71.
43. Boersma H, Wolters SL, Petrov A, et al. Minimization of infarct size with minocycline: imaging with annexin-A5 evaluation. Paper presented at: 8th International Conference of Nuclear Cardiology; May 2, 2007; Prague, Czech Republic.
44. Sarai M, Hartung D, Petrov A, et al. Broad and specific caspase inhibitor-induced acute repression of apoptosis in atherosclerotic lesions evaluated by radiolabeled annexin A5 imaging. J Am Coll Cardiol 2007;50:2305–12.
45. Muhlestein JB, Anderson JL, Cariquest JF, et al. Randomized secondary prevention trial of azithromycin in patients with coronary artery disease: Primary Clinical Results of the ACADEMIC study. Circulation 2000;102:1755–60.
46. Grayston JT, Kronmal RA, Jackson LA, et al. Azithromycin for the secondary prevention of coronary events. N Engl J Med 2005;352:1637–45.

Key Words: atherosclerosis ■ molecular imaging ■ proteinases ■ tetracyclines.